Analysis and Comparison of Several Simple Impulsive Noise Mitigation Schemes for OFDM Receivers

Sergey V. Zhidkov

***Abstract*—In this paper, we analyze and compare the performance of OFDM receivers with blanking, clipping and combined blanking-clipping nonlinear preprocessors in the presence of impulsive noise. Closed-form analytical expressions for the signal-to-noise ratio at the output of three types of nonlinearity are derived. Simulation results are provided that show good agreement with theory.**

***Index Terms*—OFDM, multicarrier modulation, impulsive noise, blanking, clipping.**

I. Introduction

ONE of the challenging problems in practical applications of digital communication techniques is reliable data transmission over wireless links in spite of man-made noise interference typical in urban environments. The man-made noise created by power lines, heavy current switches and other sources cannot be assumed to be Gaussian, and must be represented by impulsive models [1], [2].

Generally, orthogonal frequency division multiplexing (OFDM) systems are inherently robust to impulsive interference. The longer duration of OFDM symbols provide an advantage, since the impulsive noise energy is spread among simultaneously transmitted OFDM subcarriers. Nevertheless, this advantage may turn into a disadvantage if impulsive noise energy exceeds a certain threshold [3].

A simple method of reducing the adverse effect of impulsive noise is to precede a conventional OFDM demodulator with memoryless nonlinearity [4], [5], [6]. In [8], [7], it is shown that under a low signal-to-noise ratio (SNR) assumption the locally optimal detector for arbitrary signals in impulsive noise comprises of a conventional detector (optimal in Gaussian noise) preceded by a memoryless nonlinearity. Recently, the idea of using suboptimal clipping or blanking techniques for impulsive noise mitigation has been applied to modern OFDM receivers [4], [5], [6].

The aim of our study is to propose an analytical technique for performance assessment of OFDM receivers with three popular types of memoryless nonlinearity (clipping, blanking and combined clipping-blanking), and to compare the performance of these schemes in various impulsive noise scenarios. This paper provides an extension of analysis that recently appeared in [10].

Paper approved by T. F. Wong, the Editor for Wideband and Multiple Access Wireless Systems of the IEEE Communications Society. Manuscript received October 7, 2005; revised November 28, 2006.

S. V. Zhidkov is with Samsung Electronics Co., Ltd., Suwon, Korea 443-742 (e-mail: s.zhidkov@samsung.com).

Digital Object Identifier 10.1109/TCOMM.2008.050391.

II. System Model

Consider the model of the OFDM transmission system shown in fig. 1. First, in the OFDM transmitter, information bits are mapped into baseband symbols S_k using phase shift keying (PSK), or the quadrature amplitude modulation (QAM) scheme. During an active symbol interval the block of N complex baseband symbols is transformed by means of inverse discrete Fourier transform (DFT) and digital-to-analog conversion to the complex baseband OFDM signal as [12, p.719]

$$s(t) = \frac{1}{\sqrt{N}} \sum_{k=0}^{N-1} S_k e^{j\frac{2\pi kt}{T_s}}, \quad 0 < t < T_S, \tag{1}$$

where N is the number of sub-carriers, and T_S is the active symbol interval. The time-domain signal received after down-conversion, analog-to-digital conversion, and perfect synchronization can be expressed as

$$r_k = s_k + u_k, \quad k = 0, 1, ..., N-1, \tag{2}$$

where $s_k = s(kT_s/N)$ and u_k is the additive non-Gaussian noise. Without loss of generality, we assume that the signal variance is normalized to unity $\frac{1}{2}E\left[|s_k|^2\right] = \sigma_s^2 = 1$.

We also assume that the noise samples u_k are uncorrelated and their distribution can be represented using the multi-component mixture-Gaussian model [13]. In accordance with this model, the probability density function (PDF) of the noise samples (u_k) is given by

$$f(u_k) = \sum_{l=0}^{L} p_l g\left(u_k \middle| \sigma_l^2\right) \tag{3}$$

where $g\left(u_k \middle| \sigma^2\right)$ is the probability density function of the complex Gaussian variable with zero-mean and variance σ^2, and $\{\sigma_0, \sigma_1, ..., \sigma_{L-1}\}$ and $\{p_0, p_1, ..., p_{L-1}\}$ are the model parameters such that $\sum_{l=0}^{L-1} p_l = 1$.

Model (3) includes two important special cases. The first one is the two component mixture-Gaussian noise model (or ϵ - contaminated Gaussian noise model) [3]. In such a case, the model parameters can be expressed as

$$L = 2, \quad p_0 = 1-p, \quad p_1 = p, \quad \sigma_0^2 = \sigma_w^2, \quad \sigma_1^2 = \sigma_w^2 + \sigma_g^2, \tag{4}$$

where p is the probability of impulse occurrence, σ_w^2 is the additive white Gaussian noise variance, and σ_g^2 is the variance of the Gaussian component of impulsive noise (see, for example, [3]).

Another special case of (3) is the Middleton Class A interference model [1]. In this case, the model parameters can be expressed as

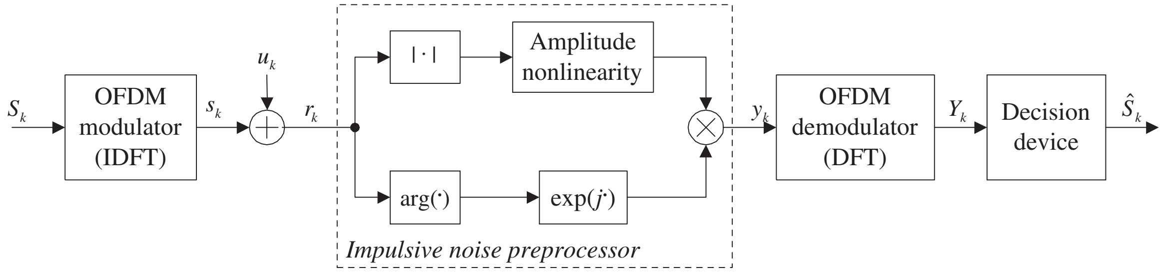

Fig. 1. Block-scheme of the OFDM transmission system with impulsive noise cancellation.

$$L=\infty,\quad p_l=\frac{e^{-A}A^l}{l!},\quad \sigma_l^2=\frac{lA^{-1}+\Gamma}{1+\Gamma}\sigma_u^2,\quad l=0,1,...,\infty \tag{5}$$

where σ_u^2 is the noise variance, A is the impulsiveness index, and Γ is the mean power ratio of the Gaussian noise component to the non-Gaussian noise component [1].

In order to reduce the adverse effect of impulsive noise, a memoryless nonlinearity can be applied at the receiver front-end of the conventional OFDM demodulator, i.e. $y_k = f(r_k)$. Note that the nonlinearity is applied to the Nyquist-rate sampled signal and therefore all distortion components fall in-band. In practical applications, the following simple nonlinearities are often used:

a) Blanking nonlinearity [4], [5]:

$$y_k=\begin{cases} r_k, & |r_k|\leqslant T\\ 0, & |r_k|>T\end{cases},\quad k=0,1,...,N-1 \tag{6}$$

where T is the blanking threshold.

b) Clipping nonlinearity [6]:

$$y_k=\begin{cases} r_k, & |r_k|\leqslant T\\ Te^{j\arg(r_k)}, & |r_k|>T\end{cases},\quad k=0,1,...,N-1 \tag{7}$$

where T is the clipping threshold.

c) Clipping/blanking nonlinearity:

$$y_k=\begin{cases} r_k, & |r_k|\leqslant T_1\\ T_1e^{j\arg(r_k)}, & T_1<|r_k|\leqslant T_2\\ 0, & |r_k|>T_2\end{cases},\quad k=0,1,...,N-1 \tag{8}$$

where T_1 is the clipping threshold and T_2 is the blanking threshold ($T_1 \leq T_2$). Note that all three nonlinearities are of amplitude type (i.e. phase of the signal is not modified); therefore, nonlinearities (6)-(8) can be represented in equivalent amplitude/phase form as illustrated in fig. 1.

After pre-processing, signal samples $\{y_k\}$ are fed to the conventional DFT-based OFDM demodulator as shown in fig. 1.

III. Signal-to-Noise Ratio at the Output of Nonlinear Preprocessor

A. SNR definition

To assess the receiver performance we shall first express the output of nonlinear preprocessor (6), (7) or (8) as

$$y_k=K_0s_k+d_k,\quad k=0,1,...,N-1, \tag{9}$$

where the first term in the right-hand side of (9) represents the scaled replica of the information-bearing signal, d_k is the cumulative noise/distortion term, and K_0 is the appropriately chosen scaling factor. Such decomposition can be justified on the basis of the extended Bussgang's theorem [11]. It is usually desirable to have zero-mean noise process d_k uncorrelated with the useful signal, i.e. $E[d_k s_k^*]=0$. It is shown [14] that the optimal scaling factor, which satisfies $E[d_k s_k^*]=0$ can be found as

$$K_0=\frac{E\left[y_k s_k^*\right]}{E\left[|s_k|^2\right]}=\frac{1}{2}E\left[y_k s_k^*\right] \tag{10}$$

The SNR at the output of memoryless nonlinearity (6), (7) or (8) can be expressed as

$$\gamma=\frac{E\left[|K_0s_k|^2\right]}{E\left[|y_k-K_0s_k|^2\right]}=\left(\frac{E_{out}}{2K_0^2}-1\right)^{-1} \tag{11}$$

where $E_{out}=E\left[|y_k|^2\right]$ represents the total signal power at the output of memoryless nonlinearity.

It should be noted that SNR (11) at the input of OFDM demodulator (DFT) and SNR at its output are equal (see [9] for proof). Note also that due to the memoryless character of nonlinearities (6)-(8) the noise process d_k is white and SNR is equal for all OFDM subchannels. The following analysis relies on the assumption that the number of OFDM subcarriers is sufficiently large ($N\to\infty$), and the OFDM signal can be modeled as a complex Gaussian process with Rayleigh envelope distribution [15].

B. SNR analysis

1) Blanking nonlinearity: Let C be the event of clipping of the signal above level T, and $\bar{C}$ be its complement. To find out K_0 and E_{out} we shall consider L mutually exclusive events I_0, I_1, ..., I_{L-1} that represent the occurrence of the noise sample with variance σ_0, σ_1, ..., σ_{L-1}, respectively. Since in blanking scheme $E\left[|y_k|^2\middle| C\right]=0$, we can express E_{out} as (12), where $P\left(\bar{C},I_l\right)=p_l\left(1-e^{-\frac{T^2}{2\left(1+\sigma_l^2\right)}}\right)$, and details of derivation of the conditional expectations $E\left[|y_k|^2\middle|\bar{C},I_l\right]$ can be found in [10].

Similarly, taking into account that for blanking nonlinearity

$$E_{out}^{(blank)} = \sum_{l=0}^{L-1} E\left[|y_k|^2 \middle| \bar{C}, I_l \right] P\left(\bar{C}, I_l\right) = 2 + 2\sum_{l=0}^{L-1} p_l \left(\sigma_l^2 - \left[\frac{T^2}{2} + \left(1+\sigma_l^2\right) \right] e^{-\frac{T^2}{2\left(1+\sigma_l^2\right)}} \right) \quad (12)$$

$E\left[y_k s_k^* \middle| C \right] = 0$, K_0 can be found as

$$K_0^{(blank)} = \frac{1}{2}\sum_{l=0}^{L-1} E\left[y_k s_k^* \middle| \bar{C}, I_l \right] P\left(\bar{C}, I_l\right) = 1 - \sum_{l=0}^{L-1} \left(1 + \frac{T^2}{2\left(1+\sigma_l^2\right)} \right) p_l e^{-\frac{T^2}{2\left(1+\sigma_l^2\right)}} \quad (13)$$

where derivation of the conditional expectations $E\left[y_k s_k^* \middle| \bar{C}, I_l \right]$ can be found in [10].

Substituting (12) and (13) in (11) yields closed-form expression for SNR at the output of blanking nonlinearity (6).

2) Clipping nonlinearity: In case of clipping nonlinearity, $E\left[|y_k|^2 \middle| C \right] \neq 0$. Therefore, the total signal power at the output of clipping nonlinearity is given by

$$E_{out}^{(clip)} = \sum_{l=0}^{L-1} E\left[|y_k|^2 \middle| \bar{C}, I_l \right] P\left(\bar{C}, I_l\right) + \sum_{l=0}^{L-1} E\left[|y_k|^2 \middle| C, I_l \right] P\left(C, I_l\right) = E_{out}^{(blank)} + \sum_{l=0}^{L-1} E\left[|y_k|^2 \middle| C, I_l \right] P\left(C, I_l\right) \quad (14)$$

where $P\left(C, I_l\right) = p_l e^{-\frac{T^2}{2\left(1+\sigma_l^2\right)}}$ and $E\left[|y_k|^2 \middle| C, I_l \right] = T^2$.

Substituting $P\left(C, I_l\right)$ and $E\left[|y_k|^2 \middle| C, I_l \right]$ and (12) into (14) yields

$$E_{out}^{(clip)} = 2 + 2\sum_{l=0}^{L-1} p_l \left(\sigma_l^2 - \left(1+\sigma_l^2\right) e^{-\frac{T^2}{2\left(1+\sigma_l^2\right)}} \right) \quad (15)$$

Similarly, $K_0^{(clip)}$ can be expressed as (16). The conditional expectation $E\left[T e^{j\arg(s_k+u_k)} s_k^* \middle| C, I_l \right]$ can be found analytically and expressed in the following closed form shown in (17) (see Appendix for details), where $Q(x)$ is the Gaussian Q-function [12, p.40]. Combining (17) and (16), we obtain (18).

3) Clipping-blanking nonlinearity: Derivations of E_{out} and K_0 for the receiver with clipping-blanking nonlinearity (8) are similar to derivations of E_{out} and K_0 for clipping nonlinearity. In this case, we shall consider the three mutually exclusive events C_0, C_1, and C_2. Event C_0 occurs when $0 < |r_k| < T_1$, event C_1 occurs when $T_1 < |r_k| < T_2$, and event C_2 occurs when $|r_k| > T_2$. Since the signal at the output of nonlinearity (8) is set to zero when $|r_k| > T_2$ (i.e. $E\left[|y_k|^2 \middle| C_2 \right] = 0$), we can express $E_{out}^{(clip/blank)}$ as shown in (19).

Similarly, K_0 for clipping-blanking nonlinearity (8) can be expressed as shown in (20). The derivation of $E\left[T_1 e^{j\arg(s_k+u_k)} s_k^* \middle| C_1, I_l \right]$ is similar to the derivation of $E\left[T e^{j\arg(s_k+u_k)} s_k^* \middle| C, I_l \right]$ for the case of clipping nonlinearity (see Appendix). After simplification, it can easily be shown that the value of $K_0^{(clip/blank)}$ can be derived from (21).

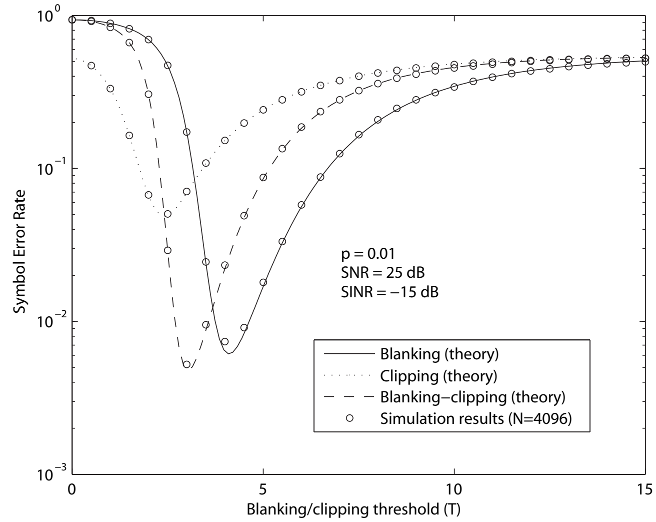

Fig. 2. Uncoded SER (16-QAM) at the output of the receiver with impulsive noise preprocessor as a function of threshold value (in case of clipping-blanking nonlinearity, $T_1 = T$ and $T_2 = 1.4T$)

As shown in [9], if the number of OFDM subcarriers is sufficiently large, noise at the input of the decision device (after DFT) can be assumed to be Gaussian. In such a case, conventional symbol/bit error rate prediction technique can be used to evaluate SER in the OFDM receiver with blanking, clipping and blanking-clipping nonlinearity. Some numerical results obtained using (11)-(21) are illustrated in Fig. 2. In this example, we have used the two-component mixture Gaussian noise model (4). The OFDM signal was scaled using estimation of $E[y_k s_k^*]$. In all figures, the input signal-to-noise ratio (SNR) is defined as $SNR = 10\log_{10}\left(1/\sigma_w^2\right)$, and the signal-to-impulsive noise ratio is defined as $SINR = 10\log_{10}\left(1/\sigma_g^2\right)$

IV. Threshold Optimization and Asymptotical Performance

Consider optimization of the threshold value(s) for nonlinearities (7)-(8). Unfortunately, the optimal threshold value(s) cannot be expressed in a simple closed form. However, numerical optimization does not introduce any difficulties and can easily be done using standard numerical software tools.

It is interesting to examine the maximum achievable SNR at the output of memoryless nonlinearities (6)-(8) that can be obtained by substituting of the numerically found optimal thresholds in (11)-(21). An example of such analysis is illustrated in Fig. 3, where the maximum achievable SNR for the three types of nonlinearity is plotted versus SINR.

As one can see, the clipping nonlinearity delivers slightly better performance than that of the blanking nonlinearity if SINR is close to 0 dB. However, when the variance of the impulsive component is increased ($SINR < -6dB$), performance of the blanking scheme improves rapidly, and asymptotically ($SINR \rightarrow -\infty$) approaches the performance

$$\begin{aligned} K_0^{(clip)} &= \frac{1}{2}\sum_{l=0}^{L-1} E\left[y_k s_k^* \middle| \bar{C}, I_l\right] P\left(\bar{C}, I_l\right) + \frac{1}{2}\sum_{l=0}^{L-1} E\left[T e^{j\arg(s_k+u_k)} s_k^* \middle| C, I_l\right] P\left(C, I_l\right) \\ &= K_0^{(blank)} + \frac{1}{2}\sum_{l=0}^{L-1} E\left[T e^{j\arg(s_k+u_k)} s_k^* \middle| C, I_l\right] P\left(C, I_l\right) \end{aligned} \quad (16)$$

$$E\left[T e^{j\arg(s_k+u_k)} s_k^* \middle| C, I_l\right] P\left(C, I_l\right) = p_l \left(\frac{T\sqrt{2\pi}}{\sqrt{1+\sigma_l^2}} Q\left(\frac{T}{\sqrt{1+\sigma_l^2}}\right) + \frac{T^2}{1+\sigma_l^2} e^{-\frac{T^2}{2\left(1+\sigma_l^2\right)}}\right) \quad (17)$$

$$K_0^{(clip)} = 1 - \sum_{l=0}^{L-1} p_l \left[e^{-\frac{T^2}{2\left(1+\sigma_l^2\right)}} - \sqrt{\frac{\pi}{2}} \frac{T}{\sqrt{1+\sigma_l^2}} Q\left(\frac{T}{\sqrt{1+\sigma_l^2}}\right)\right] \quad (18)$$

$$\begin{aligned} E_{out}^{(clip/blank)} &= E_{out}^{(blank)} + \sum_{l=0}^{L-1} E\left[\left|y_k\right|^2 \middle| C_1, I_l\right] P\left(C_1, I_l\right) \\ &= 2 + 2\sum_{l=0}^{L-1} p_l \left(\sigma_l^2 - \left(1+\sigma_l^2\right) e^{-\frac{T_1^2}{2\left(1+\sigma_l^2\right)}} - \frac{T_1^2}{2} e^{-\frac{T_2^2}{2\left(1+\sigma_l^2\right)}}\right) \end{aligned} \quad (19)$$

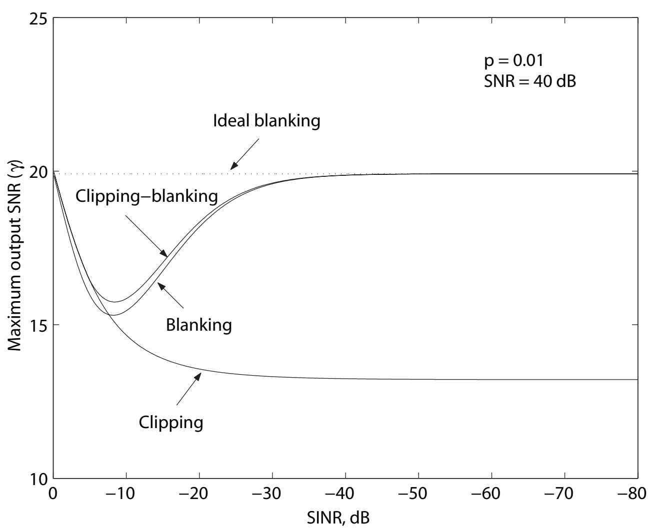

Fig. 3. Maximum achievable SNR at the output of nonlinear preprocessor as a function of SINR value

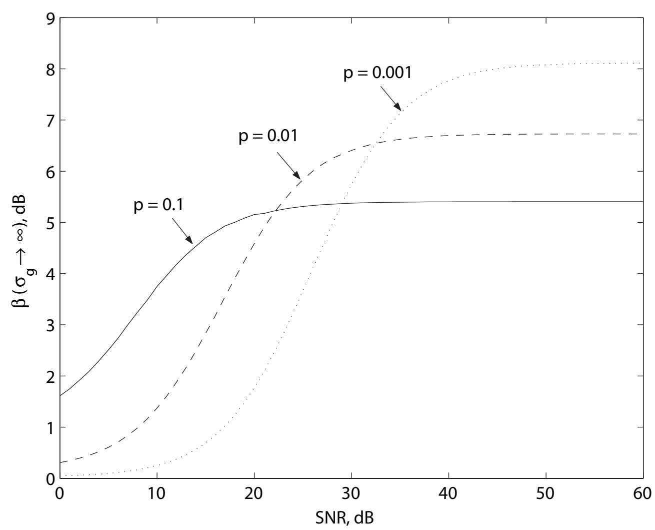

Fig. 4. Asymptotical gain of the blanking nonlinearity over clipping nonlinearity in various impulsive noise scenarios

of the ideal blanking scheme (i.e. blanking with ideal impulse detection, see [10]). On the other hand, when SINR is decreased, the performance of the clipping scheme is monotonically degraded. Clipping-blanking nonlinearity (8) with optimally selected thresholds provides the best performance.

Asymptotical improvement of the blanking scheme as compared to the clipping scheme ($\beta = \gamma^{(blank)} / \gamma^{(clip)}$) was found numerically and plotted in Fig. 4 as a function of input SNR for several probabilities of impulse occurrence p. It is seen from Fig. 4 that the blanking scheme can perform up to 6-8 dB better than the clipping scheme in severe impulsive noise scenarios.

Although the results presented in this section are for two-component mixture Gaussian noise model (4), similar results can also be obtained for the Class A impulsive noise model (5).

V. Conclusion

In this paper, closed-form expressions for the performance characterization of OFDM receivers with blanking, clipping, and combined blanking-clipping nonlinearity in the presence of impulsive noise were derived. Simulation results show that the proposed analysis provides very good prediction of the output signal-to-noise ratio (SNR). The results of this comparative study show that the blanking nonlinearity asymptotically (i.e. in highly impulsive noise) performs better than the clipping nonlinearity. On the other hand, in a weakly impulsive environment, clipping nonlinearity may slightly outperform the

$$K_0^{(clip/blank)} = K_0^{(blank)} + \frac{1}{2}\sum_{l=0}^{L-1} E\left[T_1 e^{j\arg(s_k+u_k)} s_k^* \middle| C_1, I_l\right] P\left(C_1, I_l\right) \tag{20}$$

$$\begin{aligned} K_0^{(clip/blank)} = 1 &- \sum_{l=0}^{L-1} p_l \left[e^{-\frac{T_1^2}{2\left(1+\sigma_l^2\right)}} + \frac{T_1 T_2}{2\left(1+\sigma_l^2\right)} e^{-\frac{T_2^2}{2\left(1+\sigma_l^2\right)}}\right] \\ &- \sum_{l=0}^{L-1} p_l \sqrt{\frac{\pi}{2}} \frac{T_1}{\sqrt{1+\sigma_l^2}} \left[Q\left(\frac{T_1}{\sqrt{1+\sigma_l^2}}\right) - Q\left(\frac{T_2}{\sqrt{1+\sigma_l^2}}\right)\right] \end{aligned} \tag{21}$$

blanking scheme. The best solution is, however, the clipping-blanking nonlinearity that combines the advantages of both schemes.

Appendix

A. Derivation of $E\left[Te^{j\arg(s_k+u_k)} s_k^* \middle| C, I_l\right]$

Firstly, it should be noted that the term $Te^{j\arg(s_k+u_k)} s_k^*$ can be expressed as

$$Te^{j\arg(s_k+u_k)} s_k^* = TA_s \cos\phi \tag{22}$$

where $A_s = |s_k|$, and θ is the angle between vectors s_k and r_k, i.e. $\phi = \arg(r_k) - \arg(s_k)$. Direct derivation of $E\left[TA_s\cos\phi \middle| C, I_l\right]$ is a somewhat difficult task. Conversely, $E\left[TA_s\cos\phi \middle| C, I_l\right]$ can be found indirectly using the following geometrical equality:

$$A_u^2 = A_s^2 + A_r^2 - 2A_r A_s \cos\phi \tag{23}$$

where $A_u = |u_k|$, and $A_r = |r_k|$. Multiplying both sides of (23) by T/A_r and taking expectation, we obtain

$$\begin{aligned} &E\left[TA_s\cos\phi \middle| C, I_l\right] \\ &= \frac{T}{2}\left(E\left[A_r \middle| C, I_l\right] + E\left[Z_1 \middle| C, I_l\right] + E\left[Z_2 \middle| C, I_l\right]\right) \end{aligned} \tag{24}$$

where Z_1 and Z_2 are random variables defined as $Z_1 = A_s^2/A_r$, and $Z_2 = A_u^2/A_r$. It is more convenient to find $E\left[TA_s\cos\phi \middle| C, I_l\right] P\left(C \middle| I_l\right)$ instead of $E\left[TA_s\cos\phi \middle| C, I_l\right]$. It is straightforward to show

$$\begin{aligned} &E\left[A_r \middle| C, I_l\right] P\left(C \middle| I_l\right) \\ &\quad= \int_T^\infty \frac{A_r^2}{1+\sigma_l^2} e^{-\frac{A_r^2}{2\left(1+\sigma_l^2\right)}} dA_r \\ &\quad= \sqrt{1+\sigma_l^2}\sqrt{2\pi} Q\left(\frac{T}{\sqrt{1+\sigma_l^2}}\right) + Te^{-\frac{T^2}{2\left(1+\sigma_l^2\right)}}, \end{aligned} \tag{25}$$

and

$$\begin{aligned} &E\left[Z_1 \middle| C, I_l\right] P\left(C \middle| I_l\right) \\ &= \int_T^\infty \int_0^\infty \frac{A_s^3}{\sigma_l^2} e^{-\frac{A_r^2}{2\sigma_l^2}} e^{-\frac{A_s^2}{2}\left(1+\frac{1}{\sigma_l^2}\right)} I_0\left(\frac{A_r A_s}{\sigma_l^2}\right) dA_s dA_r \\ &= \frac{2}{\left(1+\sigma_l^{-2}\right)\sigma_l^2} \int_T^\infty e^{-\frac{A_r^2}{2\left(1+\sigma_l^2\right)}} {}_1F_1\left(-1;1;-\frac{A_r^2}{2\sigma_l^2\left(1+\sigma_l^2\right)}\right) dA_r \\ &= \frac{\sqrt{2\pi}\left(2\sigma_l^4+3\sigma_l^2+1\right)}{\left(\sqrt{1+\sigma_l^2}\right)^5} Q\left(\frac{T}{\sqrt{1+\sigma_l^2}}\right) + \frac{T}{\left(1+\sigma_l^2\right)^2} e^{-\frac{T^2}{2\left(1+\sigma_l^2\right)}} \end{aligned} \tag{26}$$

and

$$\begin{aligned} &E\left[Z_2 \middle| C, I_l\right] P\left(C \middle| I_l\right) \\ &\quad= \int_T^\infty \int_0^\infty \frac{A_u^3}{\sigma_l^2} e^{-\frac{A_r^2}{2}} e^{-\frac{A_u^2}{2}\left(1+\frac{1}{\sigma_l^2}\right)} I_0\left(A_r A_u\right) dA_u dA_r \\ &\quad= \frac{\sigma_l^2\sqrt{2\pi}\left(\sigma_l^4+3\sigma_l^2+2\right)}{\left(\sqrt{1+\sigma_l^2}\right)^5} Q\left(\frac{T}{\sqrt{1+\sigma_l^2}}\right) \\ &\quad+ \frac{\sigma_l^2 T}{\left(1+\sigma_l^2\right)^2} e^{-\frac{T^2}{2\left(1+\sigma_l^2\right)}} \end{aligned} \tag{27}$$

By combining (25)-(27) and (24), simplifying, and observing that $P\left(C, I_l\right) = P\left(C \middle| I_l\right) p_l$, we can finally obtain equation (17).

References

[1] D. Middleton, "Canonical and quasi-canonical probability models of Class A interference," *IEEE Trans. Electromagn. Compat.*, vol. EMC-25, pp. 76-106, May 1983.

[2] K. L. Blackard, T. S. Rappaport, and C. W. Bostian, "Measurement and models of radio frequency impulsive noise for indoor wireless communications," *IEEE J. Sel. Areas Commun.*, vol. 11, pp. 991-1001, Sept. 1993.

[3] M. Ghosh, "Analysis of the effect of impulse noise on multicarrier and single carrier QAM systems," *IEEE Trans. Commun.*, vol. 44, no. 2, pp. 145-147, Feb. 1996.

[4] O. P. Haffenden *et al.*, "Detection and removal of clipping in multicarrier receivers," European patent application EP1043874, Oct. 11, 2000, published in Bulletin 2000/41.

[5] N. P. Cowley, A. Payne, and M. Dawkins, "COFDM tuner with impulse noise reduction," European patent application EP1180851, Feb. 20, 2002, published in Bulletin 2002/08.

[6] H. A. Suraweera, C. Chai, J. Shentu, and J. Armstrong, "Analysis of impulse noise mitigation techniques for digital television systems," in *Proc. 8th International OFDM Workshop*, Sept. 2003, pp. 172-176.

[7] S. S. Rappaport and L. Kurz, "An optimal nonlinear detector for digital data transmission through non-Gaussian channels," *IEEE Trans. Commun. Technol.*, vol. COM-14, pp. 266-274, June 1966.

[8] O. Antonov, "Optimal detection of signals in non-Gaussian noise," *Radio Eng. Electron. Phys. (USSR)*, vol. 12, pp. 541-548, 1967.

[9] J. Haring and A. J. Han Vinck, "Iterative decoding of codes over complex numbers for impulsive noise channels," *IEEE Trans. Inf. Theory*, vol. 49, no. 5, pp. 1251-1260, May 2003.

[10] S. V. Zhidkov, "Performance analysis and optimization of OFDM receiver with blanking nonlinearity in impulsive noise environment," *IEEE Trans. Veh. Technol.*, vol. 55, no. 1, pp. 234-242, Jan. 2006.

[11] D. Dardari, V. Tralli, and A. Vaccari, "A theoretical characterization of nonlinear distortion effects in OFDM systems," *IEEE Trans. Commun.*, vol. 48, no. 10, pp. 1755-1763, Oct. 2000.

[12] J. Proakis, *Digital communications*, 4th ed. McGraw-Hill, 2001.

[13] S. A. Kassam, *Signal Detection in Non-Gaussian Noise*. Berlin, Germany: Springer-Verlag, 1988.

[14] P. Banelli and S. Cacopardi, "Theoretical analysis and performance of OFDM signals in nonlinear AWGN channels," *IEEE Trans. Commun.*, vol. 48, no. 3, pp. 430-441, March 2000.

[15] S. Wei, D. L. Goeckel, and P. E. Kelly, "A modern extreme value theory approach to calculating the distribution of the peak-to-average power ratio in OFDM systems," in *Proc. IEEE Int. Conf. on Communications*, 2002, vol. 3, pp 1686-1690, April 2002.